

Experimental damage analysis of concrete structures using the vibration signature

- Part II: located damage (crack)

Z. Boukria, A. Limam

Abstract—This paper reports on an experimental non-destructive method for characterizing the damage of concrete structures using the vibration signature. The frequency of the material is an indicator of damage to the structure. The presence of cracks induces stiffness degradation in the concrete and thus causes damage. The determination of the elastic modulus and resistance characteristics of specimens through bending and compression tests is used to study the variation of dynamic modulus with characteristics of crack.

Keywords—Located damage, concrete, crack, vibration frequency, elastic modulus.

I. INTRODUCTION

FOR the safety of civil engineering structures, periodic testing is necessary. It is important for the engineer to ensure that buildings are capable of performing their function. This is possible through the detection of any weaknesses over time and the subsequent orderly planning of necessary interventions. In order to monitor these structures, it is important to be able to identifying their condition [1,2,3].

Concrete damage is the major problem for this type of structure. Its characterization has been treated by several authors using a physical model [4,5,6] such as Mazars' isotropic model [7] based on Kachanov's variable of [8]. Other authors have used non-destructive methods: dynamic testing [9,10] where the principle is to analyze the changing of dynamic characteristics [11,12,13] in the presence of damage, ultrasonic methods [14,15] based on wave propagation, or a combination of several methods [16].

Concrete is a composite material composed of aggregates of different sizes, a cement matrix and cavities. It presents randomly distributed micro-cracks which are present prior to any external stress. Depending on the nature and intensity of the stress, concrete deformation is complex [17,18] involving one or more combinations of basic mechanisms: elasticity, damage, sliding friction and cracking. This makes it difficult to find a physical model to represent these fracture modes and crack propagation that is reliable and easy to use.

This study is based on damage analysis using vibration signatures. The various methods for vibrating structures to

identify the natural frequencies of a building are easy to implement (non-destructive methods). The objective is to periodically determine the "vibration signature" of the studied specimens and correlate any changes in them subsequent to a loss in strength.

II. APPROACH

The method is based on studying dynamic modulus (Young and shear) [19,20] over time as well as diffuse defects on specimens. It consists of vibrating a cured concrete specimen, measuring the resonant frequency with Grindosonic [21] and calculating the dynamic modulus of elasticity of the specimen with the obtained results.

The GrindoSonic (Fig. 1) is a device for measuring the elastic properties of materials using a dynamic method. The speed and simplicity of these non-destructive measurements means that they can be repeated without limitation on the same specimen to observe changes over time.

The instrument uses the excitation pulse technique [22] to dynamically determine the elastic modulus of materials.



Fig. 1 Grindosonic

The operation consists of exciting the object with a light mechanical impulse and to analyze the resulting transient vibration. The natural vibration is determined by the geometry and physical properties of the specimen. A piezoelectric sensor (or microphone) is used to sense the mechanical vibration and convert it into an electrical signal. An electronic circuit detects the zero crossing, accurately marking the successive periods. As the signal decreases, the instrument measures each period and keeps the value in memory. This continues until the virtual

extinction of the signal. Finally, the microprocessor analyzes the stored information, selects the fundamental component of the spectrum and displays the measurement result.

This result may appear in 3 forms: i) the traditional reading (R) which gives the duration of two periods of the fundamental vibration, expressed in microseconds; ii) the new reading (T), which also gives the length of two periods but in a constant resolution format (this format requires the use of commas and display units on milliseconds or microseconds) and iii) the frequency (F) expressed in hertz or kilohertz.

There is a very simple relationship between reading (R or T in μs) and frequency (F in Hz):

$$F = 2,000,000 / R$$

There are three steps to performing a test: placing the sensor, impacting the specimen, and reading the measurement.

The positions of the piezoelectric sensor, the impact and the support can all be changed according to the different resonance modes.

The following figure (Fig. 2) summarizes the procedure for each mode of vibration and the formula for calculating the Young's modulus.

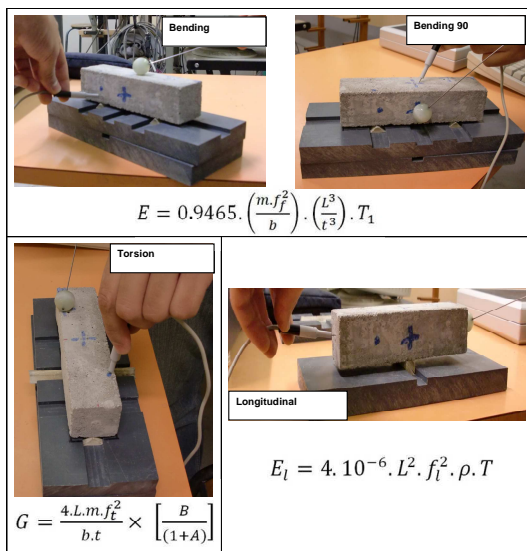


Fig. 2 Measurement of Young's modulus by Grindosonic

With this method, measurements can be made on all solid materials as long as the internal friction does not exceed a certain limit. The dimensions and shapes of objects measured can vary widely, ranging from small bars measuring 3 x 4 x 40 to concrete beams weighing over a ton.

III. EXPERIMENTAL SET-UP

To fabricate the specimens, the standard NF EN 196-1 [23] was respected for material quantities. For the tests, a reference specimen "without cracks" and 12 cracked specimens were manufactured (Fig. 3) by varying the following parameters:

- Crack width: 0.2 mm, 0.5 mm and 1 mm.
- Crack depth: 10 mm, 20 mm and 30 mm.
- Crack layout: two angles: 90 ° and 45 °

- Crack position: to define a zone of influence that is created around a crack, three distances are considered: 30mm, 100mm and 120mm
- Crack numbers: specimens with 1, 2 or 3 cracks.



Fig. 3 Manufacturing cracked specimens

The following table (Table. 1) summarizes the specimens with the dimensions and position of cracks. Each crack is characterized by the term $f_i = (e, l, d)$ with i: the number of the specimen, e: the opening (or thickness) of the crack, l: depth (or height) of the crack and d: distance from the beginning of the crack from the right-hand end of the specimen.

Specimen number	Specimen scheme	Specimen photo	Crack characteristics
F ₀			Reference specimen (Without crack)
F ₁			F ₁ = (0.2,19,100)
F ₂			F ₂ = (0.5,19,100)
F ₃			F ₃ = (1.20,100)
F ₄			F ₄ = (0.5,10,100)
F ₅			F ₅ = (0.5,29,100)
F ₆			F ₆ = (0.5,20,120)
F ₇			F ₇ = (0.5,19,30)
F ₈			F ₈ = (0.5,19,120) et (0.5,19, 30)
F ₉			F ₉ = (0.5,19,100) and (0.5,19, 30)

F ₁₀			F ₁₀ = (0.5,20,120) and (0.5,19, 100)
F ₁₁			F ₁₁ = (0.5,17,120) and (0.5,18, 100) and (0.5,19,30)
F ₁₂			F ₁₂ = (0.5,29,7,90) Shear crack with an angle of 45°, height = width = 22 mm

Table. 1 Cracked specimens characteristics

IV. RESULTS

It can be seen that specimens F0, F1, F3, F4, F6, F7, F8 and F10 follow the same curve as for the study of diffuse damage: the dynamic modulus increases sharply until the 70th hour, then the rise is more regular and moderate for 12 days; on the 34th day there is a slight decline.

In specimens F2, F5, F9, F11 and F12 the modulus does not fall on the 34th day, but continues to rise slightly.

Figure 27 represents the dynamic modulus for the 5 groups of settings and for the 4 tests (bending, bending 90, torsion, longitudinal). For every parameter, in the presence of a fault there is a greater or lesser decrease in the dynamic modulus. The presence of a shear crack (45°) gives a lower dynamic modulus. While the amplitude varies, the curves of the 4 tests have the same shape.

The next two graphs (Fig. 4) provide a comparison of the different parameters based on the reference specimen and using the percentage difference between the modulus.

From the results, one sees that:

- The largest percentages of deviation were obtained in bending and longitudinal tests.
- Differences in modulus in the presence of three cracks on a specimen (F11) and a shear crack (F12) are small in all tests.
- Because of the small difference in modulus (<14%) of the cracked specimen on the right of support (F7), this type of defect is difficult to detect with GrindoSonic.
- As soon as the number of cracks changes, significant differences of modulus appear.
- When comparing specimens with different types of cracks, bending vibration is the most suitable mode for evaluating localized damage in terms of stability and percentage difference.

The following table (Table. 2) presents the 5 groups used to study (by group parameter) the effect of cracking on dynamic modulus.

Group number	Comparison group	Parameter
1	F ₀ -F ₁ -F ₂ -F ₃	Crack opening
2	F ₀ -F ₂ -F ₄ -F ₅	Crack height
3	F ₀ -F ₂ -F ₆ -F ₇	Crack position
4	F ₀ -F ₂ -F ₈ -F ₉ -F ₁₀ -F ₁₁	Crack number
5	F ₀ -F ₂ -F ₁₂	Angle

Table. 2 Group parameter to study the effect of cracking

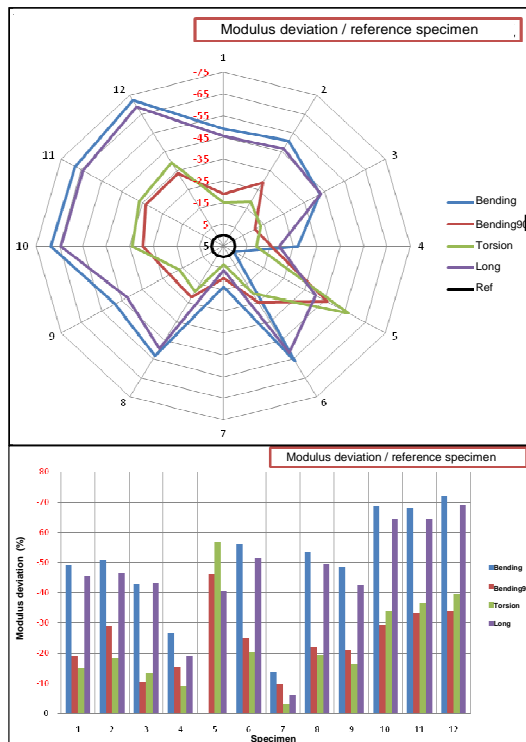


Fig. 4 Dynamic modulus - comparison with reference specimen

A. Variation of crack opening

The cracks have the same position (d = 100 mm) and the same height (l = 20 mm); only the opening varies for specimens F1, F2 and F3, respectively by 0.2, 0.5 and 1 mm. The obtained results (Fig. 5) are exploited as a graphical representation of dynamic modulus and a comparison with the reference specimen (F0).

The largest differences are in bending (18 GPa (50%)) and in the longitudinal test (1 GPa (45%)). For the difference in modulus between cracked specimens, bending 90 tests allows the characterisation of the opening (between F1 and F2: deviation of 14%).

An increase in crack opening means an increase in damage and thus a decrease (from the largest to the smallest) of the dynamic modulus.

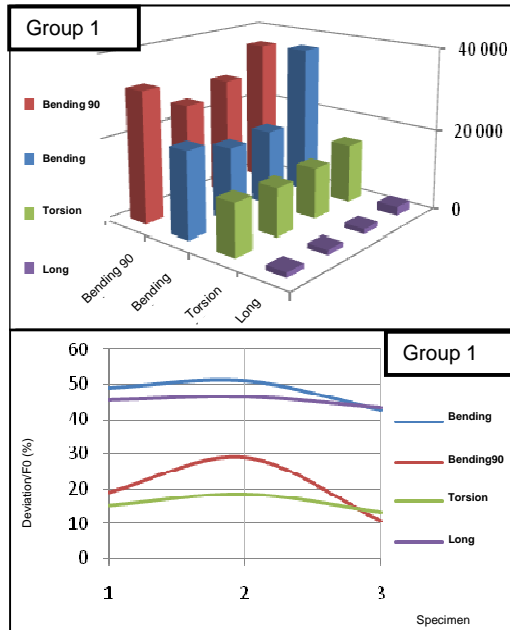


Fig 5. Dynamic modulus deviation in Group 1 compared to the reference specimen

B. Variation of crack height

The cracks have the same position ($d = 100$ mm) and the same opening ($e = 0.5$ mm); only the height varies for specimens F4, F2 and F5, respectively by 10, 20 and 25 mm. The obtained results (Fig. 6) are exploited as a graphical representation of the dynamic modulus and a comparison with the reference specimen (F0).

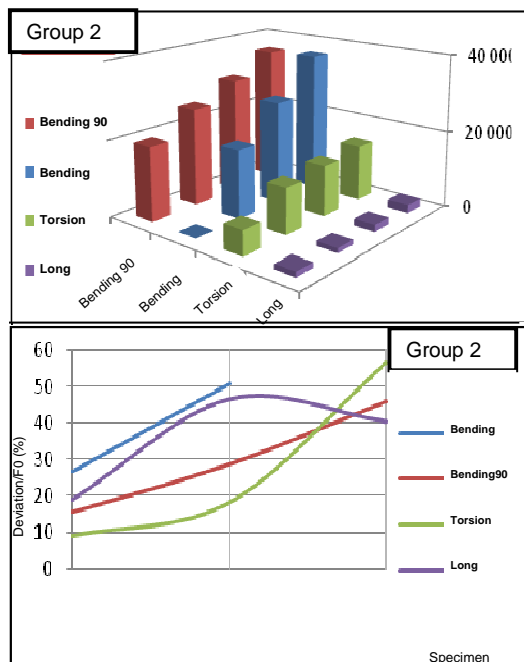


Fig. 6 Dynamic modulus deviation in Group 2 relative to the reference specimen

C. Variation of crack position

The cracks have the same height ($l = 20$ mm) and the same opening ($e = 0.5$ mm); only the position varies for specimens F6, F2 and F7, respectively by 120, 100 and 30 mm. The obtained results (Fig. 7) are exploited as a graphical representation of dynamic modulus and a comparison with the reference specimen (F0).

When the crack appears upstream of the support (F7), the deviations of dynamic modulus with respect to the reference specimen are very low. The maximum is 5 GPa, in bending, but it is negligible compared to the other two specimens, where maximum deviation is about 20 GPa.

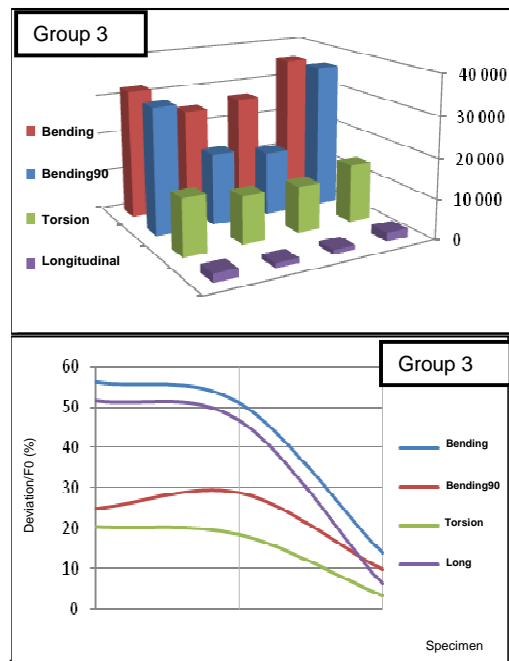


Fig. 7 Dynamic modulus deviation in Group 3 relative to the reference specimen

The more central the crack is, the lower the dynamic modulus is. But it is difficult to distinguish between specimens F2 and F6, their results being close to each other, with between 3 and 10% of variance.

The group can be divided into two parts: one consists of specimens in whom the crack is located upstream of the support and it is difficult to detect it with GrindoSonic; the other consists of specimens in whom the crack is located between the supports and its detection is easy in all tests.

D. Variation of crack number

The cracks have the same height ($l = 20$ mm) and the same opening ($e = 0.5$ mm); only the position and number of cracks varies. Specimens with two cracks are F8, F9 and F10, while specimen F11 has three cracks. The obtained results (Fig. 8) are exploited as a graphical representation of dynamic modulus and a comparison with the reference specimen (F0).

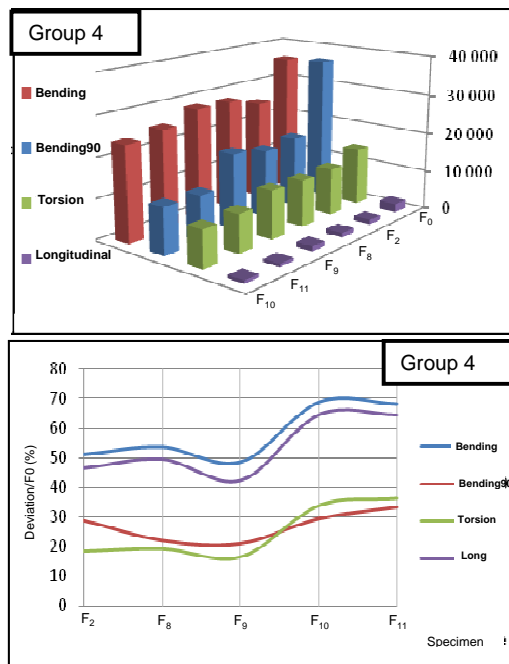


Fig. 8 Dynamic modulus deviation in Group 4 relative to the reference specimen

The dynamic modulus of specimen F2 (1 crack) are almost identical to those of specimen F9 (2 cracks with 1 upstream support). For the gap between 1 and 2 cracks to be significant, it must be positioned between the two supports. Creating a crack upstream of a support tends to conceal the appearance of a second crack from GrindoSonic. It is the same for the comparison of F10 (2 cracks between supports) with F11 (3 cracks with an upstream support); the maximum difference on various tests is a negligible 5% (Flex90) and the device did not detect the presence of the third crack.

In both cases the maximum deviation is obtained by bending at 90°. The following table shows the interest of making a comparison in bending 90: modulus differences between specimens F2, F6, F8 and F9.

	Opening	Height	Position	Number		Angle
				1 to 2	2 to 3	
Bending	*	*	+	*	+	+
Bending 90	+	+	*	+	*	-
Torsion	-	*	*	*	+	+
Longitudinal	*	*	+	*	+	+

Table. 3 Modulus comparison between the test F2, F6, F8 and F9

In the three tests, bending, torsion and longitudinal, of the 9 modulus differences, 7 are almost identical. Only the bending 90 test detects the presence of the crack upstream of the support.

It is the same for the comparison of a specimen with a crack and another with two cracks. If the second crack is upstream of the support, only the bending 90 test detects the emergence of

the second crack. Here, the difference is not great: about 10%. If the two cracks are between the two supports the largest differences are obtained with bending modulus (35%) and shear modulus (20%). The difference is negligible for the bending 90 modulus.

E. Variation of crack angle

To The results are summarized in Figure 9 which represents a modulus comparison between a specimen with a shear crack, the reference specimen and the cracked specimen F2.

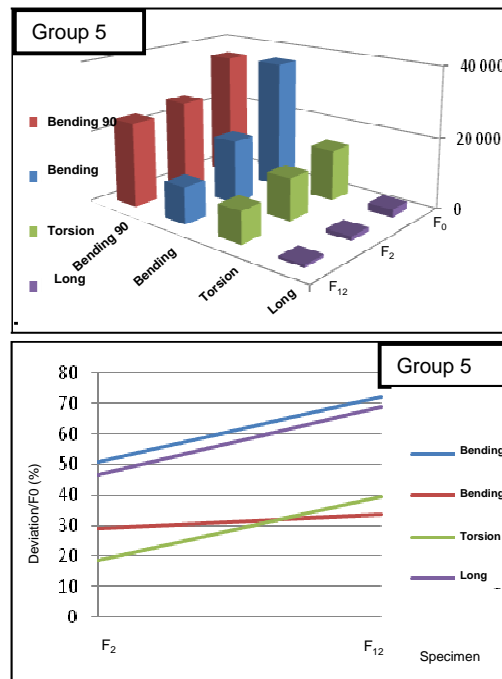


Fig. 9 Dynamic modulus deviation in Group 5 relative to the reference specimen

The presence of a shear crack provides the largest gaps: 72% difference in bending and 69% difference in longitudinal with respect to F0. When comparing the results of the perpendicular crack (F2) and the crack at 45° (F12), the variation of the gap between the modulus of the two specimens is 43% and 42% respectively.

The bending 90 test does not distinguish well between the two types of cracks, with only a 7% difference.

F. Summary of tests to be performed

Depending on the results, the four GrindoSonic tests are performed. The following table (Table. 4) summarizes the suitability of various tests according to the desired cracking criterion. For that, three levels of suitability are defined: very suitable (+), suitable (*), and largely unsuitable (-).

	Bending (MPa)	Bending 90 (MPa)	Torsion (MPa)	Longitudinal (MPa)
F2 - F6	1 749	-1 452	-1 909	109
F9 - F8	1 779	364	490	158
F2 - F6	1 851	-1 438	268	107
F9 - F8	1 826	342	391	154
F2 - F6	1 948	-1 095	461	126
F9-F8	1 942	608	477	-616

Table. 4 The suitability of various tests according to the desired cracking criterion

G. Simulation of the onset of cracking

It is interesting to study the changes in dynamic modulus by varying the cracking scenarios and knowing the boundary conditions: each simulation starts with a test on the reference specimen F0 and ends with a test on a specimen with 3 cracks: F11.

To go from 0 to 1, then to 2 and finally on to 3 cracks, 6 simulations are possible:

- Simulation 1 : $F_0 \rightarrow F_2 \rightarrow F_{10} \rightarrow F_{11}$
- Simulation 2 : $F_0 \rightarrow F_2 \rightarrow F_9 \rightarrow F_{11}$
- Simulation 3 : $F_0 \rightarrow F_6 \rightarrow F_{10} \rightarrow F_{11}$
- Simulation 4 : $F_0 \rightarrow F_6 \rightarrow F_8 \rightarrow F_{11}$
- Simulation 5 : $F_0 \rightarrow F_7 \rightarrow F_9 \rightarrow F_{11}$
- Simulation 6 : $F_0 \rightarrow F_7 \rightarrow F_8 \rightarrow F_{11}$

The simulations represented in the figure (Fig. 10) show how cracking develops

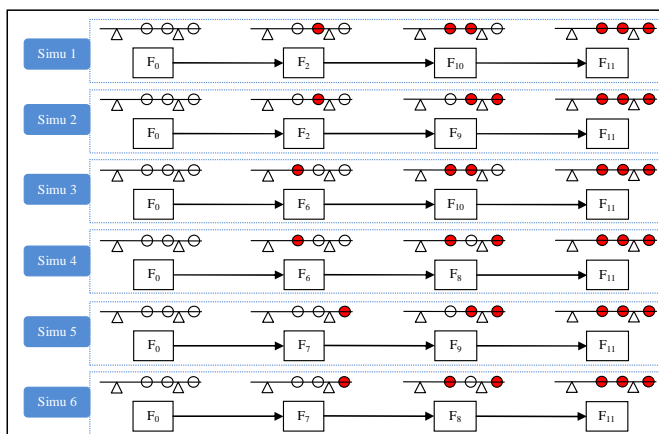


Fig. 10 Simulations of the onset of cracking

To exploit these simulations, it is possible to represent the variation of dynamic modulus for each simulation for each type of test. For bending, the results are shown in Fig. 11.

Curves are put into three groups of simulations: 1 and 3, 2 and 4, and 5 and 6.

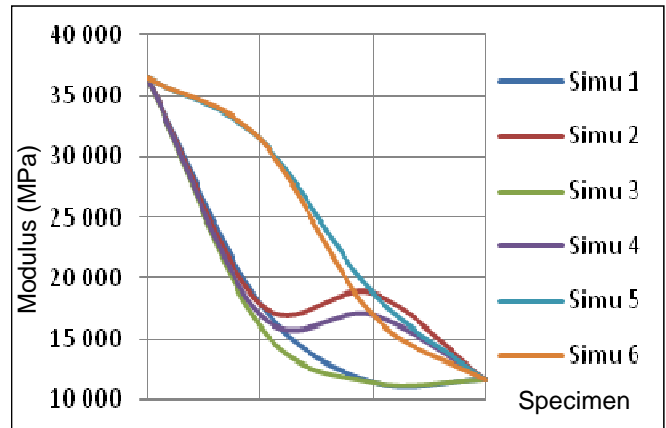


Fig. 11 Variation of flexural modulus for each simulation

In a simulation, when a crack appears upstream of a support, the modulus curve flattens out: referring to the graph of simulations 1-4, it appears that there was no defect or crack upstream.

These curves are equivalent to curves monitored over time that can be obtained using the GrindoSonic. But, while it is easy to observe that damage has occurred, it is important to complete these tests by visual inspection in order to associate defects and the drop in modulus.

V. CONCLUSION

This study has shown that the presence of crack disrupt the stability of the measurements made with GrindoSonic.

The vibration signature permits the quantification of located damage on specimens using a threshold of porosity, and to qualify located damage.

The dynamic modulus is significantly influenced by the crack characteristics, and this influence varies according to the test.

It is important to perform all the tests - bending, bending 90, longitudinal and torsion - because even if they are not well-suited to a particular type of defect, they can still be used to check the consistency of other results.

It is hoped that the present study will validate this approach through the establishment of a numerical model of the specimens designed to find the frequencies and dynamic modulus defined using GrindoSonic. The approach will then be applied to a reinforced concrete structure such as a beam or plate.

REFERENCES

- [1] BSyISO 15686 Buildings and Constructed Assets – Service Life Planning–Part 1: General Principle, British Standards Institution, London, 2000.
- [2] D. Doran, “New standard for service-life planning”. *Struct Eng*, vol. 19, no. 78. pp. 8, 2000
- [3] L.U. Litzner, “Eurocode 2-Innovations in design and construction of concrete structures”, In: R.K. Dhir. M.R. Jones (eds.), *Proceedings*

Creating with Concrete Conference, London: Thomas Telford Ltd, 2000, pp. 193–209

- [4] X. Tao, D.V. Phillips, “A simplified isotropic damage model for concrete under bi-axial stress states”, *Cement and Concrete Composites*, vol. 27, no. 6, pp. 716-726, 2005.
- [5] A. Cimetière, D. Halm, E. Molines, “A damage model for concrete beams in compression”, *Mechanics Research Communications*, vol. 34, no. 2, pp. 91-96, 2007.
- [6] A. Alliche, “Damage model for fatigue loading of concrete”, *International Journal of Fatigue*, vol. 26, no. 9, pp. 915-921, 2004
- [7] J. Mazars, “Application de la mécanique de l’endommagement au comportement non linéaire et à la rupture du béton de structure”, Thesis report, Paris 6, 1984.
- [8] L.M. Kachanov, “Time of the rupture process under creep conditions”, *Izv. Akad. Nauk. S.S.R Otd Tekh Naut*, no. 8, pp. 26-31, 1958.
- [9] N. Baghice, M. R. Esfahani, K. Moslem, “Studies on damage and FRP strengthening of reinforced concrete beams by vibration monitoring”, *Engineering Structures*, vol. 31, no. 4, pp. 875-893, 2009.
- [10] Z. Zembaty, M. Kowalski, S. Pospisil, “Dynamic identification of a reinforced concrete frame in progressive states of damage”, *Engineering Structures*, vol. 28, no. 5, pp. 668-681, 2006.
- [11] J. M. Ndambi, J. Vantomme, K. Harri, “Damage assessment in reinforced concrete beams using eigenfrequencies and mode shape derivatives”, *Engineering Structures*, vol. 24, no. 4, pp. 501-515, 2002
- [12] L. Zheng, X. Sharon Huo, Y. Yuan, “Experimental investigation on dynamic properties of rubberized concrete”, *Construction and Building Materials*, vol. 22, no. 5, pp. 939-947, 2008.
- [13] J. Maeck et al, “Damage identification in reinforced concrete structures by dynamic stiffness determination”, *Engineering Structures*, vol. 22, no. 10, pp. 1339-1349, 2000.
- [14] P. Antonaci et al, “Monitoring evolution of compressive damage in concrete with linear and nonlinear ultrasonic methods”, *Cement and Concrete Research*, vol. 40, no. 7, pp. 1106-1113, 2010.
- [15] J.F. Chaix, V. Garnier, G. Corneloup, “Concrete damage evolution analysis by backscattered ultrasonic waves”, *NDT & E International*, vol. 36, no. 7, pp. 461-469, 2003.
- [16] D. Breyse et al, “How to combine several non-destructive techniques for a better assessment of concrete structures”, *Cement and Concrete Research*, vol. 38, no. 6, pp. 783-793, 2008.
- [17] A.M. Neville, *Properties of Concrete (Fourth and Final ed.)*, John Wiley & Sons, New York, 1996.
- [18] J. M. Reynouard, G.P. Cabot, *Comportement mécanique du béton*, Editions Lavoisier, Paris, 2005.
- [19] R. Schmidt, V. Wicher, R. Tilgner, “Young’s modulus of moulding compounds measured with a resonance method”, *Polymer Testing*, 2, vol. 24, no. 2, pp. 197-203, 2005.
- [20] H. Wang, Q. Li, “Prediction of elastic modulus and Poisson’s ratio for unsaturated concrete”, *International Journal of Solids and Structures*, vol.44, no.5, pp. 1370-1379, 2007.
- [21] *GrindoSonic instrument*, available from Lemmens-Electronika, N.V. Leuven, Belgium.
- [22] *CI259-01: Standard test method for dynamic young’s modulus, Shear modulus and Poisson’s ratio for advanced ceramics by impulse excitation of vibration*, ASTM, 2001.
- [23] *NF EN 196-1. 1995 NF EN 196-1, Méthode d’essais des ciments, Partie 1: Détermination des résistances mécaniques*, 1995